

Article

LiDAR as a Tool for Assessing Change in Vertical Fuel Continuity Following Restoration

Julia H. Olszewski ^{1,2,*} and John D. Bailey ¹ ¹ College of Forestry, Oregon State University, Corvallis, OR 97331, USA; john.bailey@oregonstate.edu² Pyrologix LLC, Missoula, MT 59802, USA

* Correspondence: julia.olszewski@pyrologix.com

Abstract: The need for fuel reduction treatments and the restoration of ecosystem resilience has become widespread in forest management given fuel accumulation across many forested landscapes and a growing risk of high-intensity wildfire. However, there has been little research on methods of assessing the effectiveness of those treatments at landscape scales. Most research has involved small-scale opportunistic case studies focused on incidents where wildland fires encountered recent restoration projects. It is important to assess whether restoration practices are successful at a landscape scale so improvements may be made as treatments are expanded and their individual effectiveness ages. This study used LiDAR acquisitions taken before and after a large-scale forest restoration project in the Malheur National Forest in eastern Oregon to broadly assess changes in fuel structure. The results showed some areas where treatments appeared effective, and other areas where treatments appeared less effective. While some aspects could be modified to improve accuracy, the methods investigated in this study offer forest managers a new option for evaluating the effectiveness of fuel reduction treatments in reducing potential damage due to wildland fire.

Keywords: forest restoration; LiDAR; monitoring; canopy base height; ladder fuels



Citation: Olszewski, J.H.; Bailey, J.D. LiDAR as a Tool for Assessing Change in Vertical Fuel Continuity Following Restoration. *Forests* **2022**, *13*, 503. <https://doi.org/10.3390/f13040503>

Academic Editors: Qin Ma and Shichao Jin

Received: 9 February 2022

Accepted: 11 March 2022

Published: 24 March 2022

Publisher's Note: MDPI stays neutral with regard to jurisdictional claims in published maps and institutional affiliations.



Copyright: © 2022 by the authors. Licensee MDPI, Basel, Switzerland. This article is an open access article distributed under the terms and conditions of the Creative Commons Attribution (CC BY) license (<https://creativecommons.org/licenses/by/4.0/>).

1. Introduction

Wildland fires were actively suppressed in the United States beginning in the early 1900s given a widespread belief that fire was harmful to forests [1,2]. Cattle grazing and infrastructure built by European settlers prior to 1900 (e.g., railroad lines) also contributed to fire suppression, as the removal of surface fuels hindered subsequent spread of surface fire [3,4]. When fire is repeatedly excluded from forested ecosystems adapted to a particular fire regime [5–7], fuels and tree regeneration accumulate to a point beyond what has been historically typical [8,9]. The amount and configuration of fuels (live and dead vegetation capable of burning) has a direct effect on fire intensity and resultant severity [10,11]. Greater vertical continuity of fuels can lead to a surface fire easily spreading to the canopy above, and greater horizontal continuity of fuels can contribute to the uniform and rapid spread of a high-intensity crown fire in areas not adapted to such fire behavior [12,13].

“Restoration” has emerged as a forest management goal in many areas given the increased threat of high-intensity, high-severity wildland fire in landscapes historically subject to low-severity fire [14,15]. Restoration treatments typically involve removal of hazard fuels by prescribed fire and/or mechanical thinning appropriate to forest types and landscape positions [16–18]. Land managers prescribe such treatments to restore structural and composition of areas affected by fire exclusion. In this way, a whole suite of ecosystem services (e.g., habitat and watershed conditions) can be enhanced [19,20].

Haugo et al. [21] estimated that over four million hectares of dry forests in Washington and Oregon alone were in a state of departure from the natural range of variation. Planning restoration at a landscape scale [15] is not a simple task, as it takes cooperation from multiple stakeholders with varying agendas [22]. The Collaborative Forest Landscape Restoration

Program (CFLRP) was enacted in 2009 [23] and provides funding for collaborative groups composed of multiple stakeholders to implement large-scale projects. In the first ten years of CFLRP, a total of 5.7 million acres were treated for restoration [24].

All forest collaborative groups receiving CFLRP funding are required to conduct monitoring in order to assess the effectiveness of restoration treatments. With restoration activities conducted at a landscape scale, monitoring at a landscape scale becomes necessary [25]. Monitoring at this scale with field crews can be a challenge due to the capacity required [26] and, as a result, many forest collaborative groups have found it challenging [27].

Airborne Light Detection and Ranging (LiDAR) is a method of active remote sensing that can provide accurate forest structure data at a landscape scale [28,29], as opposed to the limited area that can be assessed with field crews. A LiDAR acquisition can be used to study forest structure at a given point in time [30,31], and multiple LiDAR acquisitions over the same area can be used to evaluate change over time. Multitemporal airborne LiDAR methods have been used to analyze the level of severity or damage following wildland fire [32,33] and resultant changes in overall forest structure [34,35]. Multitemporal airborne LiDAR may offer an opportunity to conduct landscape-scale monitoring, since it allows for the efficient collection of accurate and detailed data at a landscape scale [36].

Most forest-related use of airborne LiDAR has focused on canopy or inventory metrics [37–39]. However, primary drivers of horizontal and vertical fire spread are surface fuels, located below the canopy, and therefore, more difficult to detect using airborne LiDAR [40]. Often described as “ladder fuels”, vertical fuel continuity can increase the likelihood of a surface fire transitioning to a crown fire [41], the mitigation of which is a common goal of restoration in order to minimize fire-induced tree mortality [12].

This study addresses whether multi-temporal airborne LiDAR can be used to detect changes in two key measures of vertical fuel continuity following landscape-scale forest restoration activities. LiDAR has been employed to predict canopy base height (CBH) for use in fire modeling [28,30,42]. Ladder fuel hazard assessment class (LFHAC) is a metric developed by Menning and Stephens [43] to classify vertical fuel continuity and has been used with LiDAR data to distinguish treated areas from untreated areas [44]. CBH and LFHAC account for vertical fuel continuity in different but related ways. CBH addresses distance from the ground to the base of the canopy without accounting for surface fuels. LFHAC accounts for the distance between surface fuels and the base of the canopy. We hypothesize that these methods can effectively assess the change in vertical fuel continuity following restoration treatment across a dry forest landscape.

2. Materials and Methods

2.1. Study Area

The Damon Fuel Reduction planning area is located in the Malheur National Forest in eastern Oregon. The study area, located in the northern portion of the Damon planning area, spans an elevation gradient of 1460 m to 1650 m running from southwest to northeast. The forest types range from dry ponderosa pine (*Pinus ponderosa* Douglas ex C. Lawson) at lower elevations toward primarily mixed-conifer at higher elevations in the northeast [45]. The total area is approximately 4000 hectares. Tree species in the mixed-conifer forest type include ponderosa pine, grand fir (*Abies grandis* (Douglas ex D. Don) Lindley), and Douglas fir (*Pseudotsuga menziesii* (Mirbel) Franco). While more-moist mixed-conifer forest types tend to be more productive than the drier ponderosa pine forest type, both historically experienced a low-severity, frequent-fire regime with a mean fire return interval ranging from about 10 to 30 years [46]. Restoration treatments in the Damon planning area (Figure 1) included commercial thinning, piling and burning of residual slash, and prescribed burning [45].

Commercial thinning treatments were conducted under a variable-density silvicultural prescription in 2012, including some units thinned to enhance northern goshawk (*Accipiter gentilis atricapillus*) habitat per requirements of the Eastside Screens [45]. Mal-

heur National Forest personnel conducted a 1572-acre prescribed burn in the mixed-conifer forest type in 2014, two prescribed burns of 86 acres and 133 acres in the ponderosa pine forest type in 2016, and a 250-acre ponderosa pine forest type in 2017 that was completed prior to the beginning of the 2017 LiDAR acquisition.

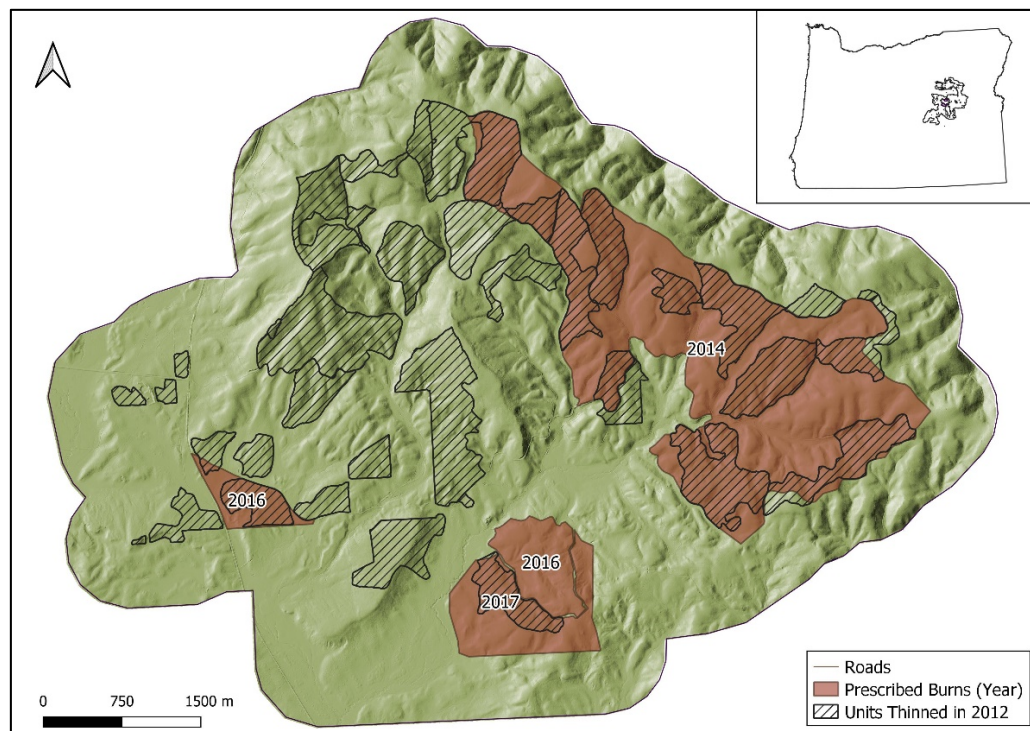


Figure 1. Map of the Damon planning area with locations and perimeters of commercial thinning treatments and prescribed burn units on the Malheur National Forest near John Day, OR, USA. The inset map shows the location of the study area and the Malheur National Forest within the state of Oregon.

2.2. Field Data

We used the area-based approach for LiDAR analysis [30] that is commonly used to predict forest attributes from LiDAR point cloud data. With this approach, field data are used to calibrate a predictive model from the LiDAR data, and the predictive model is applied to a larger landscape. Because the study area includes multiple forest types and treatment combinations, we aimed to represent all forest types and treatment combinations in the field data sample. We stratified the study area according to forest type (ponderosa and mixed conifer) and treatment combination. The four treatment combinations were: thin/prescribed burn (TB), prescribed burn (BU), thin (TH), and no treatment (NT). We randomly generated sample plot locations in ArcMap [47], with four plots in each forest type/treatment combination for a total of 32 plots (Figure 2) along with an oversample of alternate plot locations. Plots were circular with a radius of 17.84 m plus a 2-m buffer to allow for field measurement error when matching trees with LiDAR data.

We re-classified plots when they did not conform to the specified forest type (e.g., only ponderosa pine present in a designated mixed-conifer plot). If a plot did not conform to the specified treatment combination (e.g., a no-treatment plot that had been recently thinned), we either re-classified it for study purposes or rejected it in favor of an alternate plot location. If we found a plot location to be unsuitable for analysis (e.g., road or treatment boundary), it was either moved 35 m in a random direction or substituted with the nearest alternate plot.

We documented each plot center using a Trimble Nomad GPS receiver with at least 500 records, and applied differential correction using Trimble Pathfinder software, resulting

in sub-meter plot location accuracy [48]. For each tree and snag with a DBH ≥ 5.0 cm, we measured species, DBH, tree height, crown base height, bearing, and distance from plot center. We measured heights with a Haglofs hypsometer and distances with a Tru-Pulse laser rangefinder. For each plot, we assessed the LFHAC visually and took one photo in each cardinal direction from the plot center.

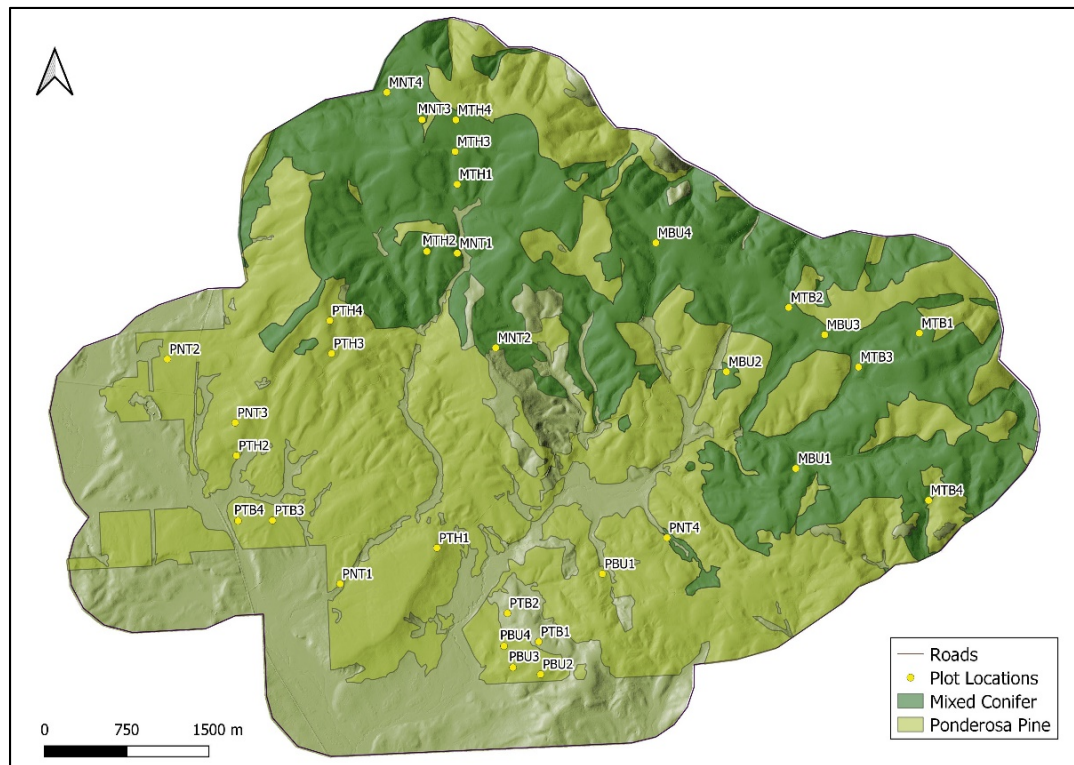


Figure 2. The study area stratified by forest type (ponderosa pine and mixed conifer) with plot locations; Malheur National Forest near John Day, OR, USA.

2.3. LiDAR Data Collection and Processing

The footprint of the 2007 LiDAR acquisition covered the entire Damon planning area, of which the study area comprises the northern portion. The footprint of the 2017 LiDAR acquisition covered a broader area that included the study area, but not the southern portion of the Damon planning area. The 2007 LiDAR data were acquired on 15 and 16 September by a Leica ALS50 Phase II laser instrument with a pulse density of 6.31 points/m² and a scan angle of $\pm 14^\circ$ from nadir by Watershed Sciences Inc. of Corvallis, OR. The 2017 LiDAR data were acquired from 14 June through 9 July with Leica ALS 80 laser instrument with a pulse density of 11.80 points/m² and a field of view of 30° by Quantum Spatial of Portland, OR. Watershed Sciences merged with two other companies in 2013 to form Quantum Spatial [49]. Horizontal and vertical conversions were applied to the 2007 data using the LAsTools las2las function [50] and NOAA VDatum [51], respectively. The 2017 data and adjusted 2007 data were compared in ArcMap to verify horizontal and vertical match. The COGO tool in ArcMap [47] was used to calculate the bearing and distance of the offset from the LiDAR-detected trees to the field-recorded trees. Then, the destpointRhum function from the R package Geosphere [52] was used to move each plot center's coordinates accordingly.

2.4. Data Analysis

All LiDAR data processing was conducted using the FUSION software program [53]. We used the ClipData function to clip the LiDAR data to the plot boundaries and subtract the elevation of the LiDAR points from the digital terrain model (DTM) to obtain height

above ground for each point. We used the FUSION function Cloudmetrics to calculate a suite of metrics based on the distribution of the height of the LiDAR returns for each of the field plots. Due to the discrepancy between the pulse densities of the two LiDAR acquisitions, we used only relative metrics such as percentage of returns and avoided absolute metrics such as number of returns. We then used the Cloudmetrics results as inputs to develop predictive models for the ladder fuel metrics. For CBH, a quantitative measure with continuous numeric values, a regression model was indicated. We used Best Subsets Regression from the R package Leaps [54] to develop a linear model based on the average CBH for each of the 32 sample plots. For LFHAC, a qualitative measure with discrete labels, a classification model was indicated. We used Random Forests with the R package RandomForests [55,56] with 500 trees and 12 variables per split. With four LFHAC observations in each of the 32 plots, 128 total observations were used in the Random Forests model. We used leave-one-out cross-validation (LOOCV) to validate the CBH model. Out-of-bag (OOB) error from the Random Forests model was used to calculate prediction error for the LFHAC model [54,57]. The goal for LFHAC was to differentiate all four classes (Table 1), but we tested combinations of classes such as high gaps/low gaps and high surface fuels/low surface fuels as well.

Table 1. Ladder fuel hazard assessment classifications, based on combination of surface fuel height and distance between surface fuels and canopy base. Adapted from Menning and Stephens [43]. High surface fuels refer to clumps of shrubs or small trees. Low surface fuels refer to a lack of clumped shrubs or small trees.

Class	Surface Fuels	Gaps
A	High	<2 m (low)
B	High	>2 m (high)
C	Low	<2 m (low)
D	Low	>2 m (high)
E	Non-Forest	Non-Forest

Kane et al. [58] suggested that LiDAR metrics (e.g., percentage of total returns) based within the 2–8 m height stratum would best represent vertical fuel continuity. Kramer et al. [44] had success with this stratum, using relative cover of LiDAR returns in the 2–4 m height stratum to differentiate treated areas from untreated. Available FUSION strata, however, are limited to two meters in height (e.g., 2–4 m, 4–6 m, etc.). For this study, we tested whether additional strata might offer a better characterization of vertical fuel continuity. We combined percentage of total LiDAR returns from individual 2-m strata to create 2–6 m, 2–8 m, 4–8 m, under 4 m, under 6 m, and under 8 m strata in addition to the standard FUSION strata.

2.5. Sample Units

Since the goal of this study was to provide fire and fuels managers with a method of assessing individual treatments, we do not draw any conclusions about which treatment type was “most effective” (*sensu* Schwilk et al., 2009). Instead, we demonstrate a process for evaluating whether stated restoration goals were achieved across a restoration landscape, a task that can be difficult with limited resources for field measurements. To accomplish this, we randomly selected one unit from each forest type/treatment combination, again seeking to represent the entire landscape. To define no-treatment units, we randomly selected from the potential vegetation GIS layer one patch of comparable size to the treatment units from each forest type. These randomly selected units will be referred to as “sample units” (Figure 3).

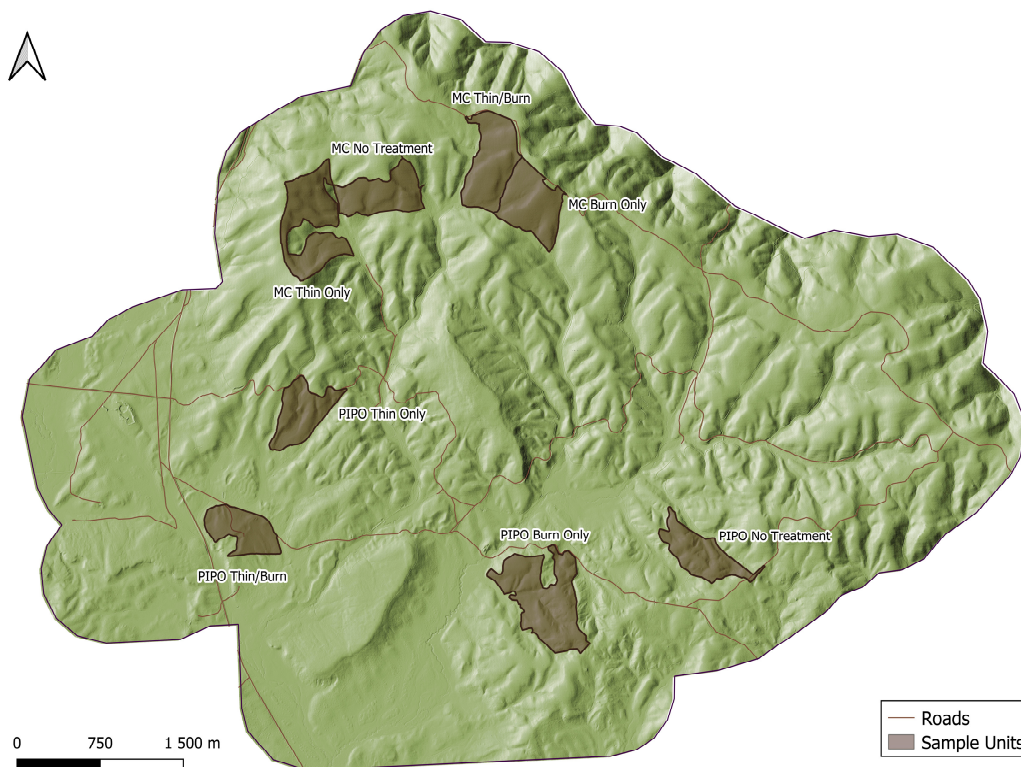


Figure 3. Sample units: randomly selected treatment and no-treatment units in ponderosa pine (PIPO) and mixed conifer (MC) forest types from the study area used to demonstrate the LiDAR-based assessment methods. Malheur National Forest near John Day, OR, USA.

We then used the FUSION function PolyClip to clip the point clouds from 2007 and 2017 to the sample unit boundaries. The FUSION function GridMetrics operates in a similar fashion to CloudMetrics but calculates outputs on a point cloud divided into a grid of individual cells rather than a point cloud clipped to plots. We selected a grid cell size of 32 m × 32 m for CBH to match plot size. Ladder fuel hazard assessment class (LFHAC) observations were made for each cardinal direction, dividing the plot size by four to create a 16 m × 16 m cell size. We calculated LiDAR metrics for each of the designated sample units in 2007 and 2017. After adding the additional 2–8 m metrics, we applied the predictive models developed from the field data and CloudMetrics results to the GridMetrics results from each sample unit in 2007 and 2017. The LiDAR metrics used in the predictive model development are listed in Appendix A Table A1. Change following treatment was calculated by comparing the 2007 results from the 2017 results. FUSION has a function, CSV2Grid, that converts the GridMetrics results from CSV to an ASCII file, which can be imported into a GIS as a raster. While we have limited the analysis to selected treatment units, a manager would have the option of assessing all treated units in a planning area, or even the entire “wall-to-wall” area covered by LiDAR.

3. Results

3.1. Canopy Base Height (CBH)

The predictive model selected from the Best Subsets Regression results is shown below in Equation (1):

$$\text{CBH} = 2.8259 + -31.3891 * \text{prop_2_6} + 0.2024 * \text{Elev.P50} + 0.1946 * \text{Elev.P80} \quad (1)$$

(adjusted R-squared = 0.6223, RMSE = 1.28)

The proportion of returns between two and six meters (prop_2_6) captures the presence of fuels between the ground and base of the canopy, the 50th percentile elevation (Elev.P50)

captures approximate canopy base height, and the 80th percentile elevation (Elev.P80) captures average tree height. Tree height is relevant as taller, older trees tend to have a higher canopy base height [12].

An increase in predicted CBH (“lift”) was detected in all sample units (Figures 4–6 and Table 2), including the no-treatment units. The mixed-conifer, thin-only unit had the smallest predicted average lift, smaller even than the mixed-conifer, no-treatment unit, while the mixed conifer burn-only unit experienced the highest predicted average lift. The predicted CBH average lift was similar for all three treated ponderosa sample units, while the predicted average CBH lift for the untreated ponderosa unit was about 0.2 m lower.

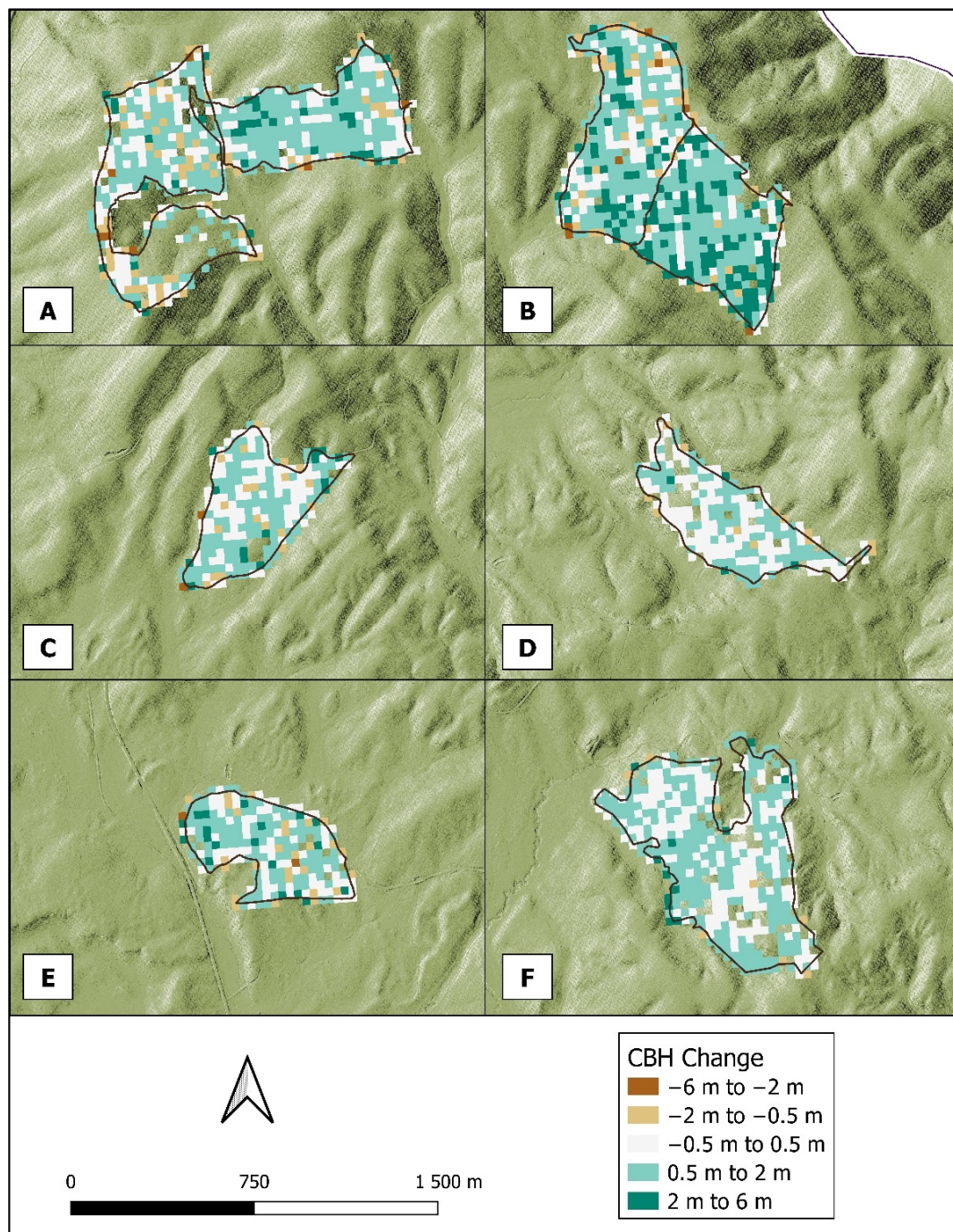


Figure 4. Predicted change in canopy base height in the sample units following fuel reduction treatments. (A) Mixed conifer TH (left) and mixed conifer NT (right). (B) Mixed conifer TB (left) and mixed conifer BU (right). (C) Ponderosa TH. (D) Ponderosa NT. (E) Ponderosa TB. (F) Ponderosa BU.

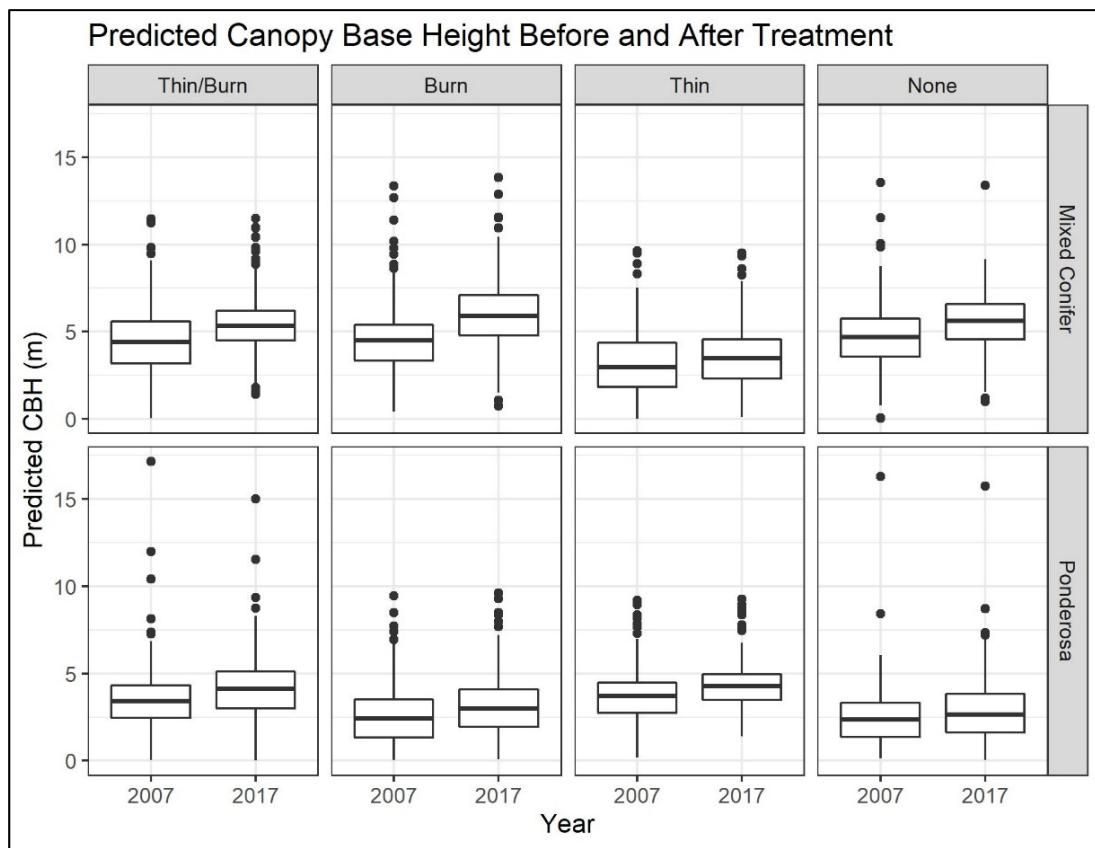


Figure 5. Predicted CBH before and after treatment in all sample units; ponderosa pine and dry mixed-conifer forest types on the Malheur National Forest near John Day, OR, USA.

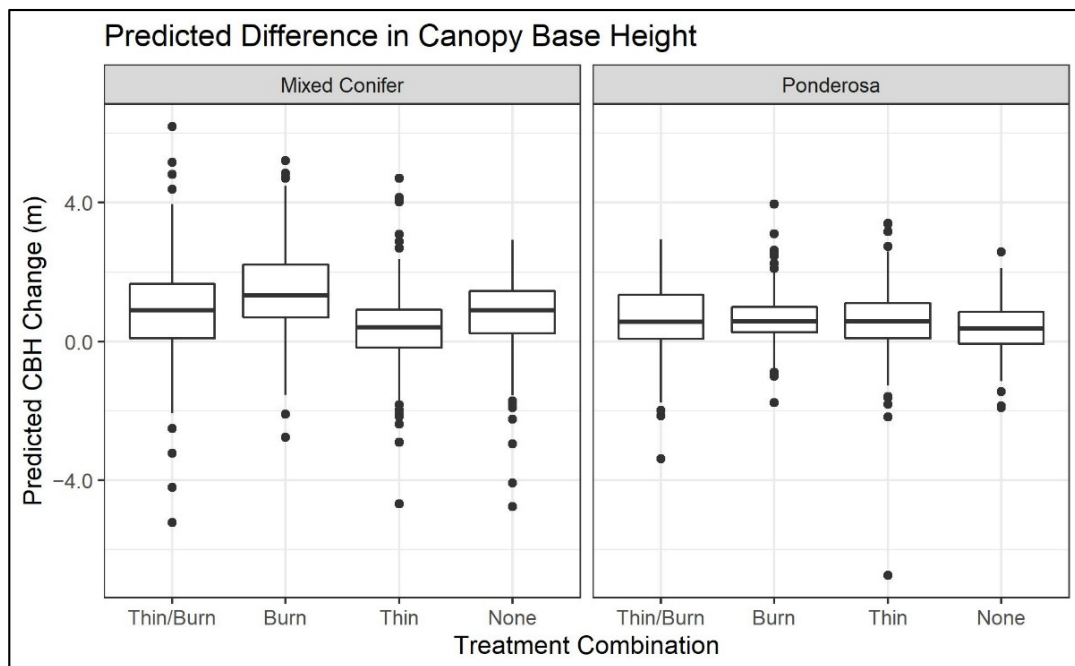


Figure 6. Predicted change in CBH in all sample units; ponderosa pine and dry mixed-conifer forest types on the Malheur National Forest near John Day, OR, USA.

Table 2. Average Canopy Base Height (CBH) by sample stand pre-/post-treatment with average 10-year change/range.

Forest Type	Treatment	Avg CBH 2007 (m)	Avg CBH 2017 (m)	Avg Change (m)	Min Change (m)	Max Change (m)
Mixed Conifer	Thin/Burn	4.42	5.31	0.89	−5.21	6.20
Mixed Conifer	Burn	4.54	5.97	1.43	−2.77	5.21
Mixed Conifer	Thin	3.18	3.55	0.36	−4.68	4.71
Mixed Conifer	None	4.76	5.56	0.80	−4.76	2.93
Ponderosa	Thin/Burn	3.56	4.18	0.62	−3.39	2.95
Ponderosa	Burn	2.51	3.16	0.66	−1.77	3.96
Ponderosa	Thin	3.73	4.32	0.60	−6.74	3.40
Ponderosa	None	2.51	2.95	0.44	−1.90	2.57

In order to account for the possibility of small patches of extreme CBH lift outweighing more widespread but less extreme lift, we also calculated the percentage of area experiencing some CBH lift (Table 3). In both mixed-conifer and ponderosa, the burn-only unit had the greatest areal extent of CBH lift. The mixed conifer burn-only unit also had the highest average predicted CBH lift. The ponderosa burn-only unit, which had a similar areal extent of predicted CBH lift as the mixed conifer burn-only unit, had a lower predicted average CBH lift than the mixed conifer burn-only unit. The mixed conifer thin-only unit had the lowest areal extent of predicted CBH lift, and it also had the lowest predicted CBH lift. The ponderosa no-treatment unit had a similar areal extent of predicted CBH lift as the mixed conifer thin-only unit.

Table 3. Percentage of area in each sample unit with a predicted CBH lift of any magnitude; ponderosa pine and dry mixed-conifer forest types on the Malheur National Forest near John Day, OR, USA.

Forest Type	Treatment	Area with Lift (%)
Mixed Conifer	Thin/Burn	77.1
Mixed Conifer	Burn	89.1
Mixed Conifer	Thin	69.4
Mixed Conifer	None	82.6
Ponderosa	Thin/Burn	75.9
Ponderosa	Burn	87.2
Ponderosa	Thin	78.3
Ponderosa	None	70.3

3.2. Ladder Fuel Hazard Assessment Class (LFHAC)

Of the individual and combined classes, the distance between surface/fuels and canopy fuels was found to have the greatest predictive power. We were unable to produce a model that adequately predicted the difference between all four classes, so we combined aspects of each class in an attempt to produce greater predictive power. Classes A and C (hereafter LoGap) both feature low gaps between the surface or surface fuels and canopy, while classes B and D (Hereafter HiGap) both feature high gaps between the surface or surface fuels and canopy. In total, 21% of LoGap grid cells were incorrectly predicted as HiGap, and 34% of the HiGap grid cells were incorrectly predicted as LoGap (Table 4). This translates to a success rate of 79% of the low gap area correctly predicted, and 66% of the high gap area is correctly predicted. The overall out-of-bag error rate from the random forests model, used in lieu of cross-validation, was 27%.

Table 4. Confusion matrix (values correctly and incorrectly predicted for field observations) for the Random Forests model to predict Ladder Fuel Hazard Assessment Class (LFHAC); Malheur National Forest near John Day, OR, USA.

	Total Observed	Predicted LoGap	Predicted HiGap	Classification Error
LoGap	62	49	13	0.21
HiGap	50	17	33	0.34

The mixed conifer thin/burn unit had the greatest predicted percentage point increase in high gaps at 30.6%. The mixed conifer burn-only and the ponderosa thin-only units both had increases of greater than 10% (Figures 7 and 8, Table 5). Both no-treatment units had a predicted decrease, and the remaining treatment stands had minimal predicted change. The ponderosa burn-only was the only treated stand that had a predicted decrease in high gaps.

Table 5. LFHAC percentages before and after treatment in each class, and percentage change before and after treatment; ponderosa pine and dry mixed-conifer forest types on the Malheur National Forest near John Day, OR, USA.

Forest Type	Treatment	2007		2017		Change
		LoGap (%)	HiGap (%)	LoGap (%)	HiGap (%)	HiGap (%)
Mixed Conifer	Thin/Burn	49.5	50.5	18.9	81.1	30.6
Mixed Conifer	Burn	45.7	54.3	32.0	68.0	13.7
Mixed Conifer	Thin	64.0	36.0	61.6	38.4	2.4
Mixed Conifer	None	41.3	58.7	45.8	54.2	−4.5
Ponderosa	Thin/Burn	53.2	46.8	49.7	50.3	3.5
Ponderosa	Burn	66.1	33.9	68.0	32.0	−1.9
Ponderosa	Thin	47.5	52.5	36.0	64.0	11.5
Ponderosa	None	68.0	32.0	75.0	25.0	−7.0

One LFHAC determination was made per cardinal direction of each plot, so the resulting cells of the GridMetrics output were one quarter of the size of the cells used for the CBH GridMetrics output. As a result, the LFHAC map is a finer grain than the CBH grid (Figure 9). Improvement in LFHAC can be seen throughout the mixed conifer thin/burn unit. A large area of no improvement from low gaps can be seen in the southern portion of the mixed conifer thin-only unit. Improvement in LFHAC can be seen scattered throughout the ponderosa thin-only and thin/burn stands, while extensive areas of no improvement from low gaps can be seen in the ponderosa no-treatment and the ponderosa burn-only stands.

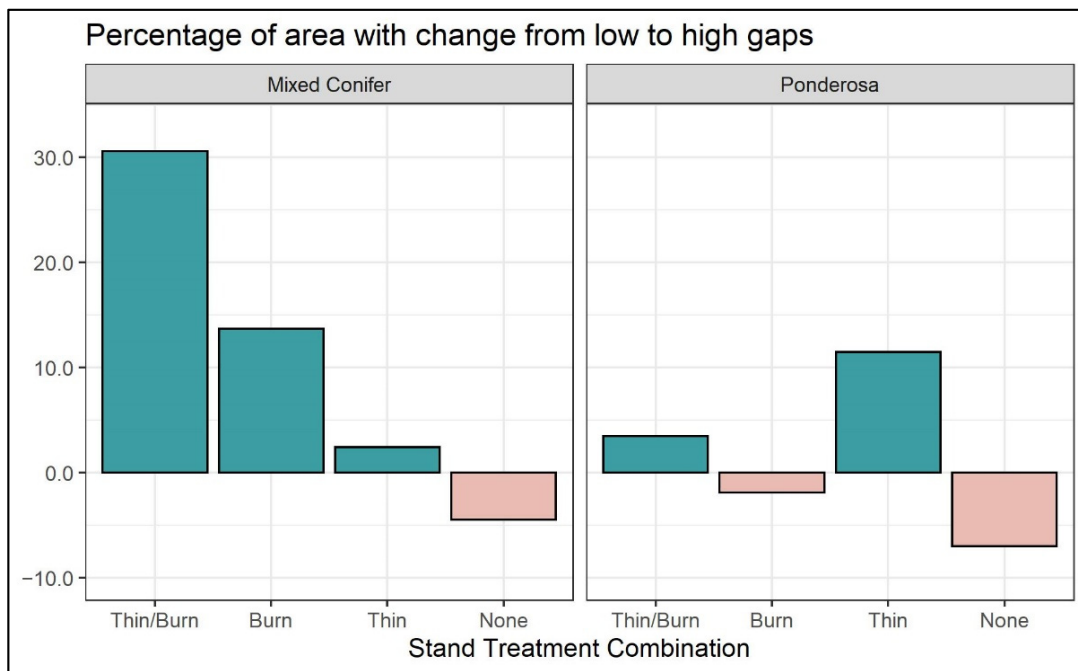


Figure 7. Percentage of area with predicted change from low gaps to high gaps in each sample unit following hazard fuel reduction; ponderosa pine and dry mixed-conifer forest types on the Malheur National Forest near John Day, OR, USA. A positive change indicates an increase in high gaps, and a negative change indicates a decrease in high gaps.

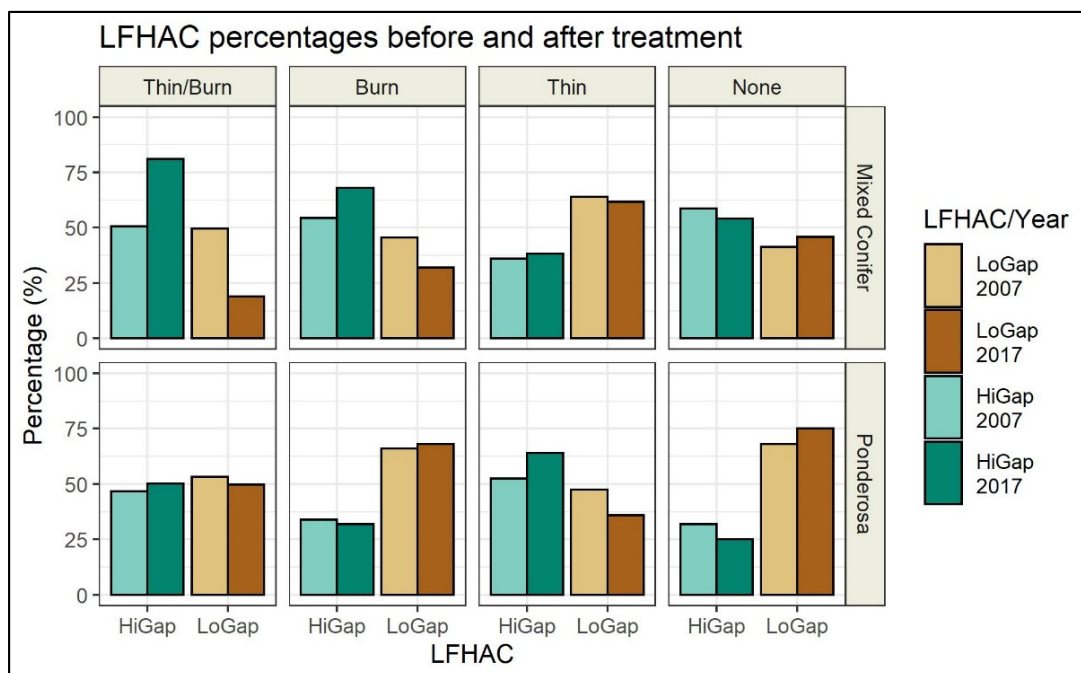


Figure 8. Predicted LFHAC before and after treatment by sample unit for ponderosa pine and dry mixed-conifer forest types on the Malheur National Forest near John Day, OR, USA.

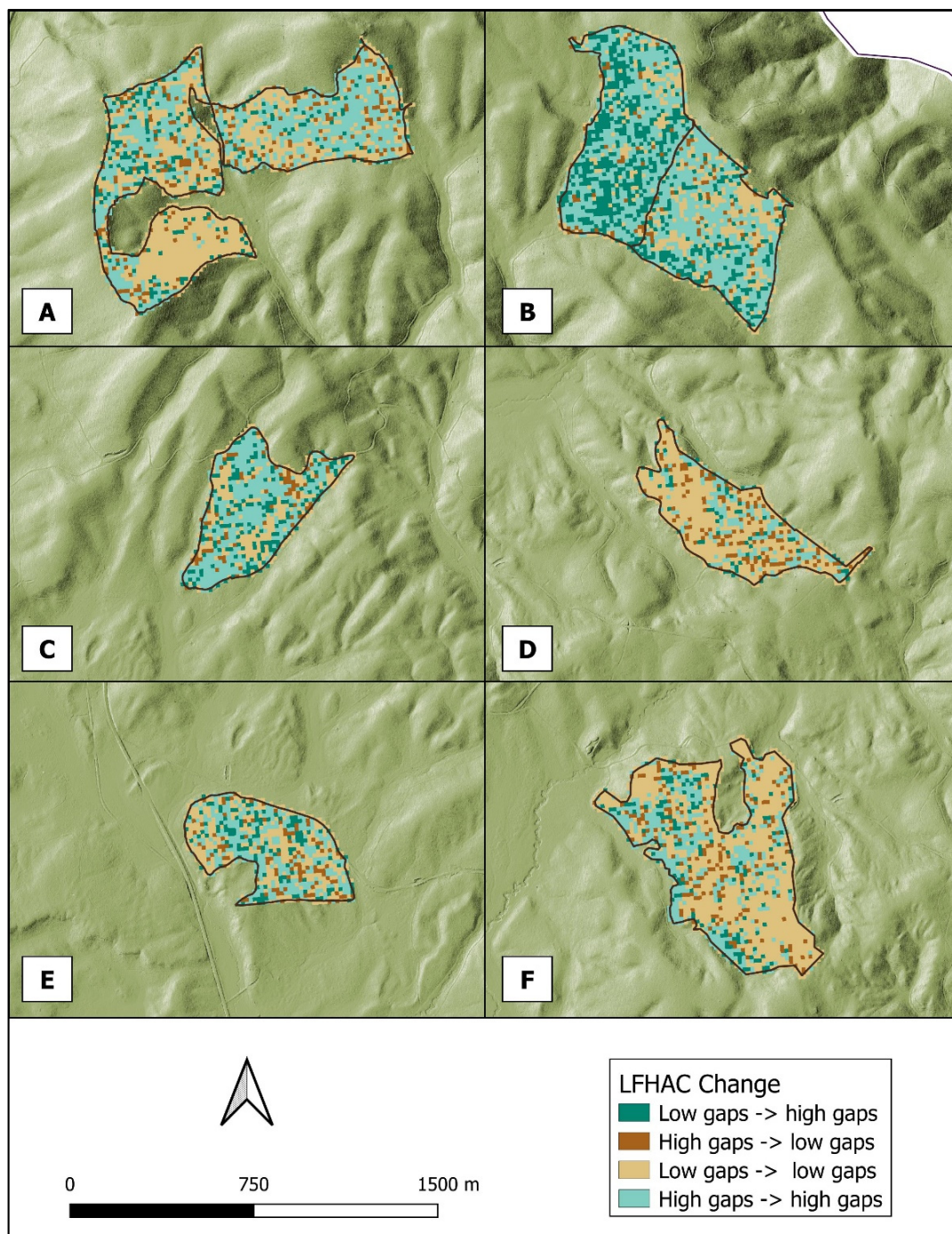


Figure 9. Predicted change in LFHAC following fuel reduction treatment in each sample unit. (A) Mixed conifer TH (left) and mixed conifer NT (right). (B) Mixed conifer TB (left) and mixed conifer BU (right). (C) Ponderosa TH. (D) Ponderosa NT. (E) Ponderosa TB. (F) Ponderosa BU.

4. Discussion

Different treatments and treatment combinations consistently influence changes in canopy base height (CBH) and ladder fuel hazard. We discuss the results from the LiDAR data here in order to illustrate what a manager might conclude about treatment effectiveness when using our methods. Prescribed fire (Figure 10) reduces surface fuels and has the potential to simultaneously lift canopies by scorching the bottom branches [12].

Thinning treatments alone likely only lift the canopy base given the tendency to remove smaller trees that have lower CBH. A thinning treatment without removal of

activity fuels may increase the surface fuel load as seen in Figure 11 and offset any gains from removing ladder fuels [59].

The mixed-conifer thin/burn treatment (Figure 12) at Damon was most effective at improving both CBH and LFHAC metrics, and it also had the highest increase in conversion of low gaps to high gaps. The mixed-conifer burn-only treatment also showed consistent success in both the CBH and LFHAC metrics, experiencing the second-highest increase in conversion of low gaps to high gaps. A manager might, therefore, conclude that such a prescription was a success and could be repeated in the future.

The mixed conifer thin-only treatment fared less well in both metrics than the two mixed-conifer units with prescribed burns, showing minimal conversion of low gaps to high gaps. Seeing such results, a manager might choose to visit the thin-only unit to examine the condition and determine whether a follow-up treatment (e.g., prescribed fire) is necessary.

Our ponderosa results at Damon were less straightforward than the mixed-conifer results. All three treated ponderosa units experienced a similar average CBH lift and area experiencing lift, with the thin/burn unit similar to the thin-only unit. Conversely, for the LFHAC metric, the ponderosa burn-only unit was the only treated unit with a decrease in high gaps. The ponderosa thin/burn unit experienced only a small increase in high gaps, while the ponderosa thin-only unit experienced a moderate increase in high gaps. Seeing these results, a manager may want to re-evaluate the ponderosa burn prescriptions or plan follow-up entries. Malheur National Forest personnel involved in the prescribed fire in the ponderosa thin/burn unit confirmed that it had burned at a relatively low intensity, leading to minimal fire effects [60].



Figure 10. An example mixed-conifer burn-only treatment in eastern Oregon, USA. Residual surface fuels are minimal and CBH is consistent with scorch marks on the tree trunks, indicating a lift in CBH due to the prescribed burn.



Figure 11. An example ponderosa pine thin-only treatment in eastern Oregon, USA. Surface fuels include abundant vegetation, including some small trees, with older surface fuel accumulations and fresh slash from the thinning treatment.



Figure 12. An example of mixed-conifer thin/burn treatment in eastern Oregon, USA. Stumps show where smaller trees were removed. Surface fuels are relatively sparse, vegetation is low and re-growing, and CBH is elevated above the ground.

Both the adjusted R-squared and RMSE are in line with studies in similar forest types that have used an area-based approach to predict CBH. Andersen et al. [28] had an RMSE of 4.1 from an unspecified type of cross-validation and an adjusted R^2 of 0.77. Hall et al. [30] reported an R^2 of 0.762 but did not conduct cross-validation. Erdody and Moskal [61] had an RMSE from cross-validation of 0.73 and an adjusted R^2 of 0.771. Jakubowski et al. [40] reported poor results for CBH in a particularly dense forest. Kramer et al. [44] found success with the same combination of classes, using a classification tree. Outside of Kramer et al. [44], who used a classification tree, there are no other known studies that have used LiDAR to predict LFHAC.

While the RMSE reported for the predicted CBH is similar to other studies, it is worth examining what the error actually captures. An error of 1.3 m could actually represent quite a range when it comes to changes in fire behavior. One meter higher or lower in CBH means a one-meter difference in the flame length capable of reaching the canopy. Many of the predicted differences in CBH were less than one meter, so a RMSE of 1.3 m means that a detected lift of less than this amount could actually be no change or a slight drop. Still, the trends shown by the results are strong enough (the CBH distributions for each stand were close to normal, indicating a central tendency) that conclusions can reasonably be drawn about the success of a treatment using this method. Similarly, the out-of-bag error rates from the Random Forests model for predicted LFHAC, at 20% and 30%, still allow a general picture of the success of treatments at a broad scale. If greater predictive accuracy is desired, it could be achieved by limiting the analysis to one treatment type or one forest type. Our aim was to show an effective assessment tool for an entire treatment landscape with all its variability. We believe this approach would show strong enough trends and consistent examples of success to be used by fire managers seeking to evaluate the effectiveness of an individual treatment. Though there are several potential sources of error in these types of analyses due to factors such as sample size and equipment limitations, general trends and impressions are often sufficient for evaluating success over broad areas. High-precision surveying equipment may not necessarily be available to a field crew with limited resources, and limited budgets may necessitate fewer validation plots than ideal. It is unlikely that the accuracy of the LiDAR data itself is a drawback, since the pulse density and accuracy of the LiDAR data used in this study is consistent with the other studies cited here.

While these methods were shown to be effective in dry, frequent-fire forests that tend to be more open, they may be less effective in denser forests [40,62]. Ladder fuels, by definition, are located below the canopy, so a thicker canopy makes characterization by LiDAR more difficult. Additionally, LiDAR can be expensive to acquire in scattered areas where it is not already available. Both pre-treatment and post-treatment LiDAR are required, and the time lapse between acquisitions could affect results as well. At seven years post-treatment, it was unclear in the mixed conifer thin-only stand whether poor results were due to an ineffective treatment or to regeneration following treatment. However, a longer time lapse allows an estimation of whether a second entry is necessary [63,64]. Another drawback to multi-temporal LiDAR is the potential need to convert the horizontal and vertical datum of one of the two acquisitions to match the other, as was the case with this study.

5. Conclusions

The methods explored in this study have been shown viable as a way to assess the effectiveness of hazard fuel reduction treatments based on the disruption of vertical fuel continuity in individual treatment units. However, potential uses of this methodology are not limited to individual stands and direct field measurements. All treatment units in any project area could be evaluated, or even the entire wall-to-wall LiDAR coverage area. Such coverage would not be possible with the small field crew typically available for such monitoring efforts. That treatment effectiveness varied among the stands underscores the need to monitor large forest restoration projects at the landscape scale [65]. Results

such as these can allow managers to adjust silvicultural (mechanical and prescribed fire) prescriptions as necessary in future treatments as well as prioritize their locations within a landscape.

While this study focused on using LiDAR data to evaluate vertical fuel continuity, additional research could identify methods using LiDAR data to assess other hazard fuel characteristics. Such characteristics could include horizontal fuel continuity or distribution of trees by size class. These methods also need not be limited to airborne LiDAR; terrestrial LiDAR is an option and may be able to gather more accurate below-canopy data [66,67]. Drone-acquired photogrammetry and structure-from-motion could also be investigated [68,69]. These emerging methods would have a much smaller footprint than airborne LiDAR but could potentially be much cheaper to acquire.

Increasingly, funding for forest restoration comes with monitoring stipulations well beyond a simple assessment of treatment acres, currently considered the requirement in most forest plans and management agencies. Funding and management directions that promote increasing size of treatment landscapes, especially as cross-boundary treatment efforts, have become more common [70] and will be necessary moving forward in order to address wildfire risk. While use in CFLRP monitoring was the original intent of this study, these methods can be used for any large-scale restoration monitoring effort.

Author Contributions: Conceptualization, methodology, analysis, and writing—original draft preparation, J.H.O. Writing—review and editing, supervision, and funding acquisition, J.D.B. All authors have read and agreed to the published version of the manuscript.

Funding: The acquisition of the LiDAR data was funded by the US Forest Service. The research was funded by the Institute for Working Forest Landscapes at Oregon State University (As an internal grant, there is no funding number).

Data Availability Statement: Not applicable.

Acknowledgments: We thank Nathan Poage for the opportunity to conduct this study, as well as Pete Heinzen and Jacob Edwards for assistance with the LiDAR data. We also thank Temesgen Hailemariam, James Johnston, Chris Dunn, and Erin Noonan for their guidance and feedback, and Audrey MacLennan and Christy Johnson for their fieldwork assistance.

Conflicts of Interest: The authors declare no conflict of interest.

Appendix A

Table A1. LiDAR metrics used to develop the predictive models for CBH and LFHAC.

LiDAR Metric	Description
Elev_max	Maximum return elevation
Elev_mean	Mean return elevation
Elev_mode	Mode return elevation
Elev_stddev	Standard deviation return elevations
Elev_variance	Variance of return elevations
Elev_CV	Coefficient of variation of return elevations
Elev_skewness	Skewness of return elevations
Elev_kurtosis	Kurtosis of return elevations
Elev_P01	1st percentile return elevation
Elev_P10	5th percentile return elevation
Elev_P20	10th percentile return elevation
Elev_P25	20th percentile return elevation
Elev_P30	25th percentile return elevation
Elev_P40	30th percentile return elevation
Elev_P50	40th percentile return elevation
Elev_P60	50th percentile return elevation
Elev_P70	60th percentile return elevation
Elev_P75	70th percentile return elevation

Table A1. Cont.

LiDAR Metric	Description
Elev_P80	75th percentile return elevation
Elev_P90	80th percentile return elevation
Elev_P95	90th percentile return elevation
Elev_P99	95th percentile return elevation
Elev_P60	99th percentile return elevation
Elev_P70	Proportion of returns below 2 m
Elev_P75	Proportion of returns between 2 m and 4 m
Elev_P80	Proportion of returns between 4 m and 6 m
Elev_P90	Proportion of returns between 6 m and 8 m
Elev_P95	Proportion of returns below 4 m
Elev_P99	Proportion of returns below 6 m
Elev_P60	Proportion of returns below 8 m
Elev_P70	Proportion of returns between 2 m and 6 m
Elev_P75	Proportion of returns between 2 m and 8 m

References

- Miller, C. The hidden consequences of fire suppression. *Park Sci.* **2011**, *28*, 75–80.
- van Wageningen, J.W. The History and Evolution of Wildland Fire Use. *Fire Ecol.* **2007**, *3*, 3–17. [[CrossRef](#)]
- Hanberry, B.B. Compositional changes in selected forest ecosystems of the western United States. *Appl. Geogr.* **2014**, *52*, 90–98. [[CrossRef](#)]
- Hessburg, P.F.; Agee, J.K.; Franklin, J.F. Dry forests and wildland fires of the inland Northwest USA: Contrasting the landscape ecology of the pre-settlement and modern eras. *For. Ecol. Manag.* **2005**, *211*, 117–139. [[CrossRef](#)]
- Higuera, P.E.; Metcalf, A.L.; Miller, C.; Buma, B.; McWethy, D.B.; Metcalf, E.C.; Ratajczak, Z.; Nelson, C.R.; Chaffin, B.C.; Stedman, R.C.; et al. Integrating Subjective and Objective Dimensions of Resilience in Fire-Prone Landscapes. *BioScience* **2019**, *69*, 379–388. [[CrossRef](#)]
- Johnstone, J.F.; Allen, C.D.; Franklin, J.F.; Frelich, L.E.; Harvey, B.J.; Higuera, P.E.; Mack, M.C.; Meentemeyer, R.K.; Metz, M.R.; Perry, G.L.W.; et al. Changing disturbance regimes, ecological memory, and forest resilience. *Front. Ecol. Environ.* **2016**, *14*, 369–378. [[CrossRef](#)]
- Stevens-Rumann, C.S.; Kemp, K.B.; Higuera, P.E.; Harvey, B.J.; Rother, M.T.; Donato, D.C.; Morgan, P.; Veblen, T.T. Evidence for declining forest resilience to wildfires under climate change. *Ecol. Lett.* **2018**, *21*, 243–252. [[CrossRef](#)]
- Fiedler, C.E.; Arno, S.F.; Harrington, M.G. Reintroducing fire in ponderosa pine-fir forests after a century of fire exclusion. In *Fire in Ecosystem Management: Shifting the Paradigm from Suppression to Prescription*. Tall Timbers Fire Ecology Conference Proceedings; Tall Timbers Research Station: Tallahassee, FL, USA, 1998; pp. 245–249.
- Lydersen, J.M.; Collins, B.M.; Knapp, E.E.; Roller, G.B. Relating fuel loads to overstorey structure and composition in a fire-excluded Sierra Nevada mixed conifer forest. *Int. J. Wildland Fire* **2015**, *24*, 484–494. [[CrossRef](#)]
- Finney, M.A.; Seli, R.C.; McHugh, C.W.; Ager, A.A.; Bahro, B.; Agee, J.K. Simulation of long-term landscape-level fuel treatment effects on large wildfires. *Int. J. Wildland Fire* **2007**, *16*, 712–727. [[CrossRef](#)]
- Keane, R.E. Describing wildland surface fuel loading for fire management: A review of approaches, methods, and systems. *Int. J. Wildland Fire* **2013**, *22*, 51–62. [[CrossRef](#)]
- Agee, J.K.; Skinner, C.N. Basic principles of forest fuel reduction treatments. *For. Ecol. Manag.* **2005**, *211*, 83–96. [[CrossRef](#)]
- Hessburg, P.F.; Churchill, D.J.; Larson, A.J.; Haugo, R.D.; Miller, C.; Spies, T.A.; North, M.P.; Povak, N.A.; Belote, R.T.; Singleton, P.H.; et al. Restoring fire-prone Inland Pacific landscapes: Seven core principles. *Landsc. Ecol.* **2015**, *30*, 1805–1835. [[CrossRef](#)]
- Brown, R.T.; Agee, J.K.; Franklin, J.F. Forest restoration and fire: Principles in the context of place. *Conserv. Biol.* **2004**, *18*, 903–912. [[CrossRef](#)]
- Stephens, S.L.; Collins, B.M.; Biber, E.; Fulé, P.Z. U.S. federal fire and forest policy: Emphasizing resilience in dry forests. *Ecosphere* **2016**, *7*, e01584. [[CrossRef](#)]
- Bailey, J.D.; Covington, W.W. Evaluating ponderosa pine regeneration rates following ecological restoration treatments in northern Arizona, USA. *For. Ecol. Manag.* **2002**, *155*, 271–278. [[CrossRef](#)]
- Fulé, P.Z.; Crouse, J.E.; Roccaforte, J.P.; Kalies, E.L. Do thinning and/or burning treatments in western USA ponderosa or Jeffrey pine-dominated forests help restore natural fire behavior? *For. Ecol. Manag.* **2012**, *269*, 68–81. [[CrossRef](#)]
- Stanturf, J.A.; Palik, B.J.; Dumroese, R.K. Contemporary forest restoration: A review emphasizing function. *For. Ecol. Manag.* **2014**, *331*, 292–323. [[CrossRef](#)]
- Franklin, J.F.; Johnson, K.N. A Restoration Framework for Federal Forests in the Pacific Northwest. *J. For.* **2012**, *110*, 429–439. [[CrossRef](#)]

20. Kalies, E.L.; Yocom Kent, L.L. Tamm Review: Are fuel treatments effective at achieving ecological and social objectives? A systematic review. *For. Ecol. Manag.* **2016**, *375*, 84–95. [[CrossRef](#)]
21. Haugo, R.; Zanger, C.; DeMeo, T.; Ringo, C.; Shlisky, A.; Blankenship, K.; Simpson, M.; Mellen-McLean, K.; Kertis, J.; Stern, M. A new approach to evaluate forest structure restoration needs across Oregon and Washington, USA. *For. Ecol. Manag.* **2015**, *335*, 37–50. [[CrossRef](#)]
22. Urgenson, L.S.; Ryan, C.M.; Halpern, C.B.; Bakker, J.D.; Belote, R.T.; Franklin, J.F.; Haugo, R.D.; Nelson, C.R.; Waltz, A.E.M. Visions of Restoration in Fire-Adapted Forest Landscapes: Lessons from the Collaborative Forest Landscape Restoration Program. *Environ. Manag.* **2017**, *59*, 338–353. [[CrossRef](#)]
23. United States Congress. *Omnibus Public Land Management Act of 2009*; Pub. L. No. 111-11, Title IV; United States Congress: Washington, DC, USA, 2009.
24. USDA Forest Service Washington Office CFLRP Staff. Collaborative Forest Landscape Restoration Program: Ten Years of Results and Lessons Learned: A Comprehensive Review of Results and Lessons Learned from Ten Years of CFLRP Implementation. 2020. Available online: https://www.fs.fed.us/restoration/documents/cflrp/CFLRP_LessonsLearnedCompiled20201016.pdf (accessed on 7 February 2022).
25. Schultz, C.A.; Coelho, D.L.; Beam, R.D. Design and governance of multiparty monitoring under the USDA Forest Service’s Collaborative Forest Landscape Restoration Program. *J. For.* **2014**, *112*, 198–206. [[CrossRef](#)]
26. Wurtzebach, Z.; Schultz, C.; Waltz, A.E.M.; Esch, B.E.; Wasserman, T.N. Broader-Scale Monitoring for Federal Forest Planning: Challenges and Opportunities. *J. For.* **2019**, *117*, 244–255. [[CrossRef](#)]
27. Esch, B.E.; Waltz, A.E.M. Assessing metrics of landscape restoration success in Collaborative Forest Landscape Restoration Projects. In *ERI White Paper—Issues in Forest Restoration*; Ecological Restoration Institute, Northern Arizona University: Flagstaff, AZ, USA, 2019.
28. Andersen, H.E.; McGaughey, R.J.; Reutebuch, S.E. Estimating forest canopy fuel parameters using LIDAR data. *Remote Sens. Environ.* **2005**, *94*, 441–449. [[CrossRef](#)]
29. Reutebuch, S.E.; Andersen, H.-E.; McGaughey, R.J. Light Detection and Ranging (LIDAR): An Emerging Tool for Multiple Resource Inventory. *J. For.* **2005**, *103*, 286–292. [[CrossRef](#)]
30. Hall, S.A.; Burke, I.C.; Box, D.O.; Kaufmann, M.R.; Stoker, J.M. Estimating stand structure using discrete-return lidar: An example from low density, fire prone ponderosa pine forests. *For. Ecol. Manag.* **2005**, *208*, 189–209. [[CrossRef](#)]
31. Richardson, J.J.; Moskal, L.M. Strengths and limitations of assessing forest density and spatial configuration with aerial LiDAR. *Remote Sens. Environ.* **2011**, *115*, 2640–2651. [[CrossRef](#)]
32. Hoe, M.S.; Dunn, C.J.; Temesgen, H. Multitemporal LiDAR improves estimates of fire severity in forested landscapes. *Int. J. Wildland Fire* **2018**, *27*, 581. [[CrossRef](#)]
33. McCarley, T.R.; Kolden, C.A.; Vaillant, N.M.; Hudak, A.T.; Smith, A.M.S.; Wing, B.M.; Kellogg, B.S.; Kreidler, J. Multi-temporal LiDAR and Landsat quantification of fire-induced changes to forest structure. *Remote Sens. Environ.* **2017**, *191*, 419–432. [[CrossRef](#)]
34. Duncanson, L.; Dubayah, R. Monitoring individual tree-based change with airborne lidar. *Ecol. Evol.* **2018**, *8*, 5079–5089. [[CrossRef](#)]
35. Marinelli, D.; Paris, C.; Bruzzone, L. A Novel Approach to 3-D Change Detection in Multitemporal LiDAR Data Acquired in Forest Areas. *IEEE Trans. Geosci. Remote Sens.* **2018**, *56*, 3030–3046. [[CrossRef](#)]
36. Wasserman, T.N.; Sánchez Meador, A.J.; Waltz, A.E.M. Grain and Extent Considerations Are Integral for Monitoring Landscape-Scale Desired Conditions in Fire-Adapted Forests. *Forests* **2019**, *10*, 465. [[CrossRef](#)]
37. Edson, C.; Wing, M.G. Airborne Light Detection and Ranging (LiDAR) for Individual Tree Stem Location, Height, and Biomass Measurements. *Remote Sens.* **2011**, *3*, 2494–2528. [[CrossRef](#)]
38. Hudak, A.T.; Evans, J.S.; Smith, A.M.S. LiDAR utility for natural resource managers. *Remote Sens.* **2009**, *1*, 934–951. [[CrossRef](#)]
39. Sheridan, R.D.; Popescu, S.C.; Gatzliolis, D.; Morgan, C.L.S.; Ku, N.W. Modeling forest aboveground biomass and volume using airborne LiDAR metrics and forest inventory and analysis data in the Pacific Northwest. *Remote Sens.* **2015**, *7*, 229–255. [[CrossRef](#)]
40. Jakubowski, M.K.; Guo, Q.; Collins, B.; Stephens, S.; Kelly, M. Predicting Surface Fuel Models and Fuel Metrics Using Lidar and CIR Imagery in a Dense, Mountainous Forest. *Photogramm. Eng. Remote Sens.* **2013**, *79*, 37–49. [[CrossRef](#)]
41. Tappeiner, J.C.; Maguire, D.A.; Harrington, T.B.; Bailey, J.D. Chapter 11: Fire and Silviculture. In *Silviculture and Ecology of Western U.S. Forests*; Oregon State University Press: Corvallis, OR, USA, 2015; pp. 316–348.
42. Chamberlain, C.P.; Sánchez Meador, A.J.; Thode, A.E. Airborne lidar provides reliable estimates of canopy base height and canopy bulk density in southwestern ponderosa pine forests. *For. Ecol. Manag.* **2021**, *481*, 118695. [[CrossRef](#)]
43. Menning, K.M.; Stephens, S.L. Fire Climbing in the Forest: A Semiquantitative, Semiquantitative Approach to Assessing Ladder Fuel Hazards. *West. J. Appl. For.* **2007**, *22*, 88–93. [[CrossRef](#)]
44. Kramer, H.; Collins, B.; Kelly, M.; Stephens, S. Quantifying Ladder Fuels: A New Approach Using LiDAR. *Forests* **2014**, *5*, 1432–1453. [[CrossRef](#)]
45. Malheur National Forest. Damon Wildland Urban Interface Project—Environmental Assessment. 2010. Available online: https://www.fs.usda.gov/nfs/11558/www/nepa/47110_FSPLT1_025758.pdf (accessed on 7 February 2022).
46. Johnston, J.D.; Bailey, J.D.; Dunn, C.J. Influence of fire disturbance and biophysical heterogeneity on pre-settlement ponderosa pine and mixed conifer forests. *Ecosphere* **2016**, *7*, e01581. [[CrossRef](#)]
47. ESRI. ArcMap. (Version 10.6) [Software]. 2018. Available online: <http://desktop.arcgis.com/en/arcmap/> (accessed on 7 February 2022).

48. Trimble. Trimble GPS Pathfinder Office. Trimble Geospatial. 2018. Available online: <https://geospatial.trimble.com/products-and-solutions/gps-pathfinder-office> (accessed on 7 February 2022).
49. PRWeb. Quantum Spatial Formed through Merger of AeroMetric, Photo Science and WSI. 2013. Available online: <https://www.prweb.com/releases/2013/9/prweb11086471.htm> (accessed on 6 January 2019).
50. Rapidlasso. LAStools. [Software]. 2018. Available online: <https://rapidlasso.com/LAStools/> (accessed on 7 February 2022).
51. NOAA. VDatum. (Version 3.9). [Software]. 2018. Available online: <https://www.vdatum.noaa.gov/> (accessed on 7 February 2022).
52. Hijmans, R. Geosphere. (R Package Version 1.5-7). [Software]. 2017. Available online: <https://cran.r-project.org/web/packages/geosphere/index.html> (accessed on 7 February 2022).
53. McGaughey, R. FUSION. (Version 3.80). [Software]. 2018. Available online: <http://forsys.cfr.washington.edu/fusion/fusionlatest.html> (accessed on 7 February 2022).
54. Lumley, T.; Miller, A. Leaps: Regression Subset Selection. R Package Version 3.0. [Software]. 2017. Available online: <https://cran.r-project.org/web/packages/leaps/index.html> (accessed on 7 February 2022).
55. Breiman, L. Random forests. *Mach. Learn.* **2001**, *45*, 29. [CrossRef]
56. Liaw, A.; Wiener, M. Classification and Regression by randomForest. *R News* **2002**, *2*, 18–22. Available online: <https://cran.r-project.org/doc/Rnews/> (accessed on 7 February 2022).
57. Breiman, L.; Cutler, A. (n.d.) Random Forests: Balancing Prediction Error. [Web]. Available online: https://www.stat.berkeley.edu/~breiman/RandomForests/cc_home.htm (accessed on 7 February 2022).
58. Kane, V.R.; North, M.P.; Lutz, J.A.; Churchill, D.J.; Roberts, S.L.; Smith, D.F.; McGaughey, R.J.; Kane, J.T.; Brooks, M.L. Assessing fire effects on forest spatial structure using a fusion of Landsat and airborne LiDAR data in Yosemite National Park. *Remote Sens. Environ.* **2014**, *151*, 89–101. [CrossRef]
59. Youngblood, A.; Wright, C.S.; Ottmar, R.D.; McIver, J.D. Changes in fuelbed characteristics and resulting fire potentials after fuel reduction treatments in dry forests of the Blue Mountains, northeastern Oregon. *For. Ecol. Manag.* **2008**, *255*, 3151–3169. [CrossRef]
60. Clark, E.; (Malheur National Forest, USDA Forest Service). Personal Communication, 17 October 2019.
61. Erdody, T.L.; Moskal, L.M. Fusion of LiDAR and imagery for estimating forest canopy fuels. *Remote Sens. Environ.* **2010**, *114*, 725–737. [CrossRef]
62. Stefanidou, A.; Gitas, I.Z.; Korhonen, L.; Stavrakoudis, D.; Georgopoulos, N. LiDAR-Based Estimates of Canopy Base Height for a Dense Uneven-Aged Structured Forest. *Remote Sens.* **2020**, *12*, 1565. [CrossRef]
63. Stephens, S.L.; Collins, B.M.; Roller, G. Fuel treatment longevity in a Sierra Nevada mixed conifer forest. *For. Ecol. Manag.* **2012**, *285*, 204–212. [CrossRef]
64. Vaillant, N.M.; Noonan-Wright, E.K.; Reiner, A.L.; Ewell, C.M.; Rau, B.M.; Fites-Kaufman, J.A.; Dailey, S.N. Fuel accumulation and forest structure change following hazardous fuel reduction treatments throughout California. *Int. J. Wildland Fire* **2015**, *24*, 361–371. [CrossRef]
65. Hummel, S.; Hudak, A.T.; Uebler, E.H.; Falkowski, M.J.; Megown, K.A. A comparison of accuracy and cost of LiDAR versus stand exam data for landscape management on the Malheur National Forest. *J. For.* **2011**, *109*, 267–273. [CrossRef]
66. Donager, J.J.; Sankey, T.T.; Sankey, J.B.; Sanchez Meador, A.J.; Springer, A.E.; Bailey, J.D. Examining Forest Structure With Terrestrial Lidar: Suggestions and Novel Techniques Based on Comparisons Between Scanners and Forest Treatments. *Earth Space Sci.* **2018**, *5*, 753–776. [CrossRef]
67. LaRue, E.A.; Wagner, F.W.; Fei, S.; Atkins, J.W.; Fahey, R.T.; Gough, C.M.; Hardiman, B.S. Compatibility of aerial and terrestrial LiDAR for quantifying forest structural diversity. *Remote Sens.* **2020**, *12*, 1407. [CrossRef]
68. Cunliffe, A.M.; Brazier, R.E.; Anderson, K. Ultra-fine grain landscape-scale quantification of dryland vegetation structure with drone-acquired structure-from-motion photogrammetry. *Remote Sens. Environ.* **2016**, *183*, 129–143. [CrossRef]
69. Iglhaut, J.; Cabo, C.; Puliti, S.; Piermattei, L.; O'Connor, J.; Rosette, J. Structure from Motion Photogrammetry in Forestry: A Review. *Curr. For. Rep.* **2019**, *5*, 155–168. [CrossRef]
70. Charnley, S.; Kelly, E.C.; Fischer, A.P. Fostering collective action to reduce wildfire risk across property boundaries in the American West. *Environ. Res. Lett.* **2020**, *15*, 025007. [CrossRef]